Computation of the electromagnetic pion form factor from lattice QCD in the ϵ regime

H. Fukaya,[1] S. Aoki,[2,3] S. Hashimoto,[4,5] T. Kaneko,[4,5] H. Matsufuru,[4,5] and J. Noaki[4]

(JLQCD Collaboration)

[1]*Department of Physics, Osaka University, Toyonaka 560-0043, Japan*
[2]*Yukawa Institute for Theoretical Physics, Kyoto University, Kyoto 606-8502, Japan*
[3]*Center for Computational Sciences, University of Tsukuba, Tsukuba, Ibaraki 305-8577, Japan*
[4]*KEK Theory Center, High Energy Accelerator Research Organization (KEK), Tsukuba 305-0801, Japan*
[5]*School of High Energy Accelerator Science, The Graduate University for Advanced Studies (Sokendai),
Tsukuba 305-0801, Japan*

We calculate the electromagnetic pion form factor in lattice QCD with $2 + 1$ flavors of the dynamical overlap quarks. Up and down quark masses are set below their physical values so that the system is in the so-called ϵ regime with the small size of our lattice ~ 1.8 fm. The finite volume corrections are generally expected to be $\sim 100\%$ in the ϵ regime. We, however, find a way to automatically cancel the dominant part of them. Inserting nonzero momenta and taking appropriate ratios of the two- and three-point functions, we can eliminate the contribution from the zero-momentum pion mode. Then the remaining finite volume effect is a small perturbation from the nonzero modes. Our lattice data agree with this theoretical prediction and the extracted pion charge radius is consistent with the experiment.

I. INTRODUCTION

Dynamics of pions is governed by its nature as the Nambu-Goldstone boson associated with the spontaneous breaking of chiral symmetry in the vacuum of quantum chromodynamics (QCD). Beyond the leading order in the expansion in terms of pion momentum squared p^2 and pion mass squared m_π^2, it develops a nonanalytic functional form [1,2] known as the chiral logarithm. For the charged pion form factor $F_V(q^2)$ as a function of the momentum transfer q, in particular, the charge radius defined by

$$\langle r^2 \rangle_V \equiv 6 \frac{\partial F_V(q^2)}{\partial q^2}\bigg|_{q^2=0} \qquad (1)$$

is predicted to diverge in the limit of vanishing pion mass, i.e., $\sim \ln m_\pi^2$. In order for numerical computations of lattice QCD to be reliable in reproducing the low-energy property of the pions, it is crucial to confirm this remarkable behavior.

In the lattice QCD simulations, approaching the chiral limit is challenging because the computational cost to invert the Dirac operator grows as $1/m_\pi^2$. Furthermore, finite volume effect is expected to increase as m_π decreases. Therefore, to avoid large systematic effect from the volume, the overall cost increases much faster than $1/m_\pi^2$. Most of the previous calculations, including our own work [3], have been performed at large pion masses ($\gtrsim 300$ MeV), and the results for the pion charge radius were significantly lower than the experimental value. Recent works [4–6] are

simulating lighter pions and the results are indeed showing an increase towards the physical pion mass. However, in the vicinity of the chiral limit, the violation of chiral symmetry becomes an issue with the conventional lattice fermion formulations, such as the Wilson fermions. They violate the chiral symmetry at the order of $a^2 \Lambda_{\text{QCD}}^3$ [assuming the $O(a)$-improved action], where Λ_{QCD} (~ 300 MeV) is the typical scale of QCD. In the most recent dynamical simulations, the lattice cutoff $1/a$ is around 3 GeV, and the size of the violation is thus an order of 3 MeV, which is only slightly below the physical up and down quark masses. This implies that in the quark mass regime we are interested in, the violation of chiral symmetry due to the lattice artifact is as large as in magnitude the effect due to the quark mass. A discretization effect in such a situation could become sizable.

In this work we carry out a lattice calculation of the pion charge radius near the chiral limit using the fermion formulation that preserves exact chiral symmetry [7]. We simulate lattice QCD with up and down quark masses below the physical point, employing the overlap fermion action [9,10]. This overlap fermion action has an exact chiral symmetry through the Ginsparg-Wilson relation [11,12]. In our numerical implementation, this relation is kept at the level of 10^{-8} accuracy. Therefore, the chiral logarithm is expected to have the same functional form as the continuum theory. By obtaining a data point with an extremely small pion and combining it with our previous results at a larger mass region, we make an interpolation into the physical point. This *chiral interpolation* can

suppress the systematic error from the mass dependence of the data, and confirm if there is the expected divergent behavior of the pion charge radius.

At the small quark mass (~ 3 MeV), the finite volume effect is expected to be quite large for the lattice size (~ 1.8 fm) that we use. It is often mentioned in the literature [13] that $m_\pi L$ has to be larger than 4 in order to suppress the finite volume effect at a few percent levels or lower. At our simulated pion mass, L must be as large as 5–6 fm to satisfy this criterion. In the regime where the near-zero modes determine the dynamics, however, the dominant part of the finite volume effects come from the zero-momentum mode of the pions, while the higher energy states give still exponentially small effects. (Note that the energy of nonzero momentum modes in a finite volume satisfies $E_\pi > 2\pi/L$, and thus, $E_\pi L > 6$.) Therefore, once we remove the effect of the pion zero-momentum mode, the remaining finite volume effect is manageable. For this purpose, the so-called ϵ expansion [14–17] was developed and applied to extract the low-energy constants of chiral perturbation theory (ChPT).

The ϵ expansion is valid for a system where the pion Compton wavelength exceeds L. In this ϵ regime, the zero-momentum mode may rotate in the flavor group manifold $SU(N_f)$ and therefore, should be treated nonperturbatively. Such analysis leads to the prediction of the low-lying Dirac operator eigenvalue spectrum [18–22], as well as the pseudoscalar two-point functions [23,24]. These formulas have rather complicated expressions containing Bessel functions, but nicely describe the lattice data [25–35], and are useful to determine the leading two low-energy constants, the chiral condensate Σ, and pion decay constant F.

In order to extract the pion form factor from the ϵ regime lattice calculation, we need the ChPT prediction of the three-point functions, which is not known in the literature, except for the kaon sectors [36–38]. Even if such predictions were available, the analysis would require a nontrivial task to disentangle the low-energy physics from some complicated form of the Bessel functions coming from the zero mode.

In this work, we would like to show a new direction, using the ϵ expansion in a more indirect way. Namely, we use the ϵ expansion of ChPT just for finding the combination of the correlators which has a small sensitivity to the volume. We find that this is possible by inserting nonzero momenta to the relevant operators (or simply taking differences of them at different time slices), and taking appropriate ratios of them. This procedure automatically eliminates the leading $\mathcal{O}(1)$ finite volume effects, and the remaining next-to-leading order (NLO) contributions are expected to be a small perturbation [39,40].

This method considerably simplifies the analysis in the ϵ regime. Since the dominance of the pion zero-mode contribution in the finite volume effect is universal for most correlators, we expect that the application of the method is wider, e.g., other meson/baryon form factors. Even in the p regime, our method suggests a way to minimize the finite volume effects. In this work, we present the result for the electromagnetic pion form factor as the first example. Our lattice data for the electromagnetic form factor agree with this theoretical expectation reasonably well, yielding a consistent value of the pion charge radius with the experiment.

This paper is organized as follows. In Sec. II, we revisit the two-point functions in the ϵ regime of ChPT and demonstrate how our new strategy works to automatically cancel the dominant finite volume effects of the pion zero mode. In Sec. III, we compute the ϵ expansion of the three-point functions and find the ratios of the correlators which are free from the pion zero mode's contamination. The result of our simulation is presented in Sec. IV and we give our conclusion in Sec. V.

II. TWO-POINT FUNCTIONS IN THE ϵ REGIME

Let us consider the two-point correlators to illustrate our idea. For simplicity, we consider two-flavor ChPT with a degenerate quark mass m in a finite volume $V = L^3 T$, of which the boundary condition is set periodic in every direction. Let us denote the chiral condensate by Σ and the pion decay constant by F. Including the (sea) strange quark is not difficult [41] and does not change the following results at the leading order of ChPT.

In the ϵ expansion of ChPT, the pion's zero-momentum mode is exactly treated by performing a group integral over $SU(N_f)$, where $N_f = 2$ is the number of flavors, while the nonzero modes and their interactions are perturbatively treated. Namely, it is a (weakly coupled) system of $SU(2)$ matrix model [or a $U(2)$ matrix model when the global topological charge of the gauge field is fixed] and massless fields.

A two-point correlation function of pseudoscalar density operator $P(x)$ separated by a four vector $x = (t, x_1, x_2, x_3)$ is expressed as [41]

$$\langle P(x)P(0)\rangle = X + Y\left(\frac{1}{V}\sum_{p\neq 0}\frac{e^{ipx}}{p^2}\right)$$
$$+ Z\left(\frac{1}{V}\sum_{p\neq 0}\frac{e^{ipx}}{(p^2)^2}\right) + \cdots, \qquad (2)$$

where $X, Y, Z, \ldots$ are nontrivial (Bessel) functions of $m\Sigma V$ arising from the zero-mode integrals. Unlike the conventional meson propagator, there is a constant term X, which is a contribution purely from the zero mode. The second and third terms represent the coupled contribution of the zero modes to the nonzero modes described as a massless scalar field. It is massless because the mass term is a small perturbation in the ϵ expansion. Note that the $p = 0$ part contribution is absent in the momentum summations

and this expression is manifestly free from infrared divergences.

Since the nonzero modes are treated as massless bosons, the correlation function projected onto zero spatial momentum becomes a polynomial function of t, which is a remarkable difference from the conventional exponential function $\exp(-m_\pi t)$ in the conventional p regime. In fact, this special property of the ϵ expansion was used to extract the low-energy constants from finite volume lattice QCD [28,30,32,42]. In this work we try to avoid the terms arising from the zero-mode integral, which is characteristic of the ϵ regime.

In fact, Eq. (2) can be written in a different form

$$\langle P(x)P(0)\rangle = X + Y\left(\frac{1}{V}\sum_{p\neq 0}\frac{e^{ipx}}{p^2 + m_\pi^2 + \Delta m_\pi^2}\right) + \cdots,$$

$$\Delta m_\pi^2 = -Z/Y - m_\pi^2, \qquad (3)$$

of which the difference from the original Eq. (2) is the next-to-next-to-next-to-leading order. By a direct calculation of the zero mode [40], one can show

$$\lim_{m\Sigma V\to\infty}\Delta m_\pi^2 = 0, \qquad \lim_{m\Sigma V\to 0}\Delta m_\pi^2 = \frac{2}{F^2 V}. \qquad (4)$$

This expression suggests that if we can remove X and Y, the remaining correlator looks almost the same as that in the conventional p regime, except for a perturbative correction to the pion mass. Note that even though the relative correction to the pion mass is $\mathcal{O}(1)$ its influence to the correlator is small since the conditions $p^2 \gg m_\pi^2$ and $p^2 \gg \Delta m_\pi^2$ are kept for any p^2 in a finite volume.

FIG. 1 (color online). Ratio, $C_{PP}^{2\mathrm{pt}}(t,\mathbf{p})/\Delta_t C_{PP}^{2\mathrm{pt}}(t,\mathbf{0})$, of two-point correlators at different momenta where we set $t_{\mathrm{ref}} = 16$. Lattice data are plotted together with the expectation of ChPT at the leading order without mass (ignoring Z) (solid curve) and with mass $(m_\pi^2 + \Delta m_\pi^2)^{1/2} = 100$ MeV (dashed curve). Different symbols represent $\mathbf{p} = (1,0,0), (1,1,0), (1,1,1),$ and $(2,0,0)$ in units of $2\pi/L$. Here, the rotationally symmetric correlators are averaged in the data.

We proceed as follows. First, we insert a spatial momentum $\mathbf{p}$ and subtract the correlator at a different time slice t_{ref} in the case of $\mathbf{p} = \mathbf{0}$:

$$C_{PP}^{2\mathrm{pt}}(t,\mathbf{p}) \equiv \int d^3x e^{-i\mathbf{p}\cdot\mathbf{x}}\langle P(x)P(0)\rangle, \qquad (5)$$

$$\Delta_t C_{PP}^{2\mathrm{pt}}(t,\mathbf{0}) \equiv C_{PP}^{2\mathrm{pt}}(t,\mathbf{0}) - C_{PP}^{2\mathrm{pt}}(t_{\mathrm{ref}},\mathbf{0}), \qquad (6)$$

and then, take a ratio of them,

$$\frac{C_{PP}^{2\mathrm{pt}}(t,\mathbf{p})}{\Delta_t C_{PP}^{2\mathrm{pt}}(t,\mathbf{0})} = \frac{E(\mathbf{0})\sinh(E(\mathbf{0})T/2)}{E(\mathbf{p})\sinh(E(\mathbf{p})T/2)} \times \frac{\cosh(E(\mathbf{p})(t - T/2))}{\cosh(E(\mathbf{0})(t - T/2)) - \cosh(E(\mathbf{0})(t_{\mathrm{ref}} - T/2))}, \qquad (7)$$

where $E(\mathbf{p}) = \sqrt{\mathbf{p}^2 + m_\pi^2 + \Delta m_\pi^2}$. Note that this ratio is finite even in the limit $E(\mathbf{0}) = 0$. We can thus eliminate the leading zero mode's contributions X and Y in (3). Here, t_{ref} should be taken as large as possible to avoid the contamination from the excited states, provided the data at t_{ref} is statistically reliable.

In order to validate the idea based on the form (3) we make a plot of the ratio $C_{PP}^{2\mathrm{pt}}(t,\mathbf{p})/\Delta_t C_{PP}^{2\mathrm{pt}}(t,\mathbf{0})$ with $t_{\mathrm{ref}} = 16$, for different momenta $\mathbf{p}$ in Fig. 1, and compare with its expectation at the leading order in the ϵ expansion in solid (neglecting Z) and dashed [we input $(m_\pi^2 + \Delta m_\pi^2)^{1/2} = 100$ MeV] curves. The solid curves, at the leading order of ChPT neglecting Z, have no free parameter to tune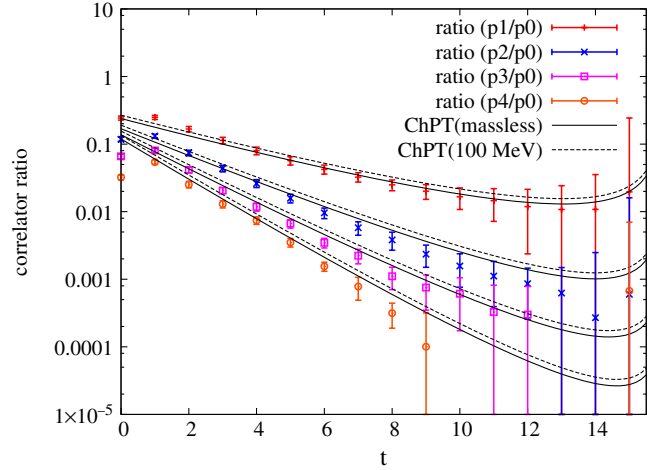, as they are simply constructed from massless propagators. The agreement of the lattice data with the expectation is fairly good. Also, we can see that the difference from the massive correlators is tiny, although some deviations are seen in higher momentum correlators, which may imply momentum dependent higher-order corrections from nonzero modes. This good agreement indicates that the dominant part of the finite size effect or the peculiarity of the ϵ regime is eliminated, and the remaining nontrivial NLO contribution coming from the Z term is small compared to the statistical fluctuation.

III. THREE-POINT FUNCTIONS IN THE ϵ REGIME

In this section, we apply the idea of eliminating the zero-mode contribution to the three-point function. For this

purpose, we first consider the ϵ expansion of the pion form factor within the framework of ChPT, since the finite volume effect is dominated by the lightest degrees of freedom, i.e., the pion. In the physical pion form factor, on the other hand, the contribution beyond the leading terms of the ϵ expansion becomes important as suggested by the fact the vector pole dominance $1/(1 - q^2/m_V^2)$ describes the data quite well [3,43]. Such higher-order contributions are irrelevant to the study of the leading finite volume effect considered in this work.

It is straightforward to extend the analysis of the two-point function described in the previous subsection to the case of three-point function. It is expressed as a series, of which each term is a product of the constant due to zero-mode integrals and the massless propagators of the ξ field such that they connect to form the three-point function. When the propagator must carry nonzero momentum, the constant term due to the zero-mode integral cannot arise.

In the case of our "pseudoscalar-(zero-component) vector-pseudoscalar" correlator, the series is expressed by

$$\langle P(x)V_0(y)P(z)\rangle = A\frac{1}{V}\sum_{p\neq 0}\frac{ip_0}{p^2}\left(e^{ip(x-y)} + e^{ip(y-z)}\right)$$

$$+ B\frac{1}{V^2}\sum_{p\neq 0}\sum_{p'\neq 0}\frac{(ip_0 + ip_0')e^{ip(x-y)}e^{ip'(y-z)}}{p^2 p'^2}F_V((p-p')^2) + \cdots, \tag{8}$$

where $F_V(q^2)$ denotes the vector form factor of the pion (which is equivalent to our target electromagnetic form factor when the up and down quarks are degenerate), and A, $B, \ldots$ are dimensionful constants, including the contributions from the pion zero mode.

Inserting an initial (spatial) momentum $\mathbf{p}_i$ to $P(x)$, and a final momentum $\mathbf{p}_f$ to $P(z)$, we define a three-point function

$$C_{PVP}^{3\text{pt}}(t, t'; \mathbf{p}_i, \mathbf{p}_f) \equiv \int d^3x\, e^{-i\mathbf{p}_i\cdot\mathbf{x}}$$

$$\times \int d^3z\, e^{i\mathbf{p}_f\cdot\mathbf{z}}\langle P(x)V_0(y)P(z)\rangle, \tag{9}$$

where we assume $t = x_0 - y_0 < T/2$, and $t' = y_0 - z_0 < T/2$. As in the discussion of the two-point function, we then define a difference operator $\Delta_t f(t) = f(t) - f(t_{\text{ref}})$ with a fixed value of t_{ref}. It should not be confused with the conventional derivative operator ∂_t. Here, the choice for t_{ref} is more restricted than in the case of two-point functions, since it should satisfy both of $t + t_{\text{ref}} \ll T$ and $t' + t_{\text{ref}} \ll T$ to avoid the contribution of the unusual modes wrapping around the lattice. In the following analysis, we choose $t_{\text{ref}} = T/3 = 12$, and use the data at $t < t_{\text{ref}}$ and $t' < t_{\text{ref}}$.

We construct the following three ratios:

$$R_V^1(t, t'; |\mathbf{p}_i|, |\mathbf{p}_f|, q^2) \equiv \frac{\frac{1}{N_{|\mathbf{p}_i|,|\mathbf{p}_f|}^{3\text{pt}}}\sum_{\text{fixed}|\mathbf{p}_i|,|\mathbf{p}_f|,q^2}\frac{C_{PVP}^{3\text{pt}}(t,t';\mathbf{p}_i,\mathbf{p}_f)}{E(\mathbf{p}_i)+E(\mathbf{p}_f)}}{\left(\frac{1}{N_{|\mathbf{p}_i|}^{2\text{pt}}}\sum_{\text{fixed}|\mathbf{p}_i|}C_{PP}^{2\text{pt}}(t,\mathbf{p}_i)\right)\left(\frac{1}{N_{|\mathbf{p}_f|}^{2\text{pt}}}\sum_{\text{fixed}|\mathbf{p}_f|}C_{PP}^{2\text{pt}}(t',\mathbf{p}_f)\right)}, \tag{10}$$

$$R_V^2(t, t'; |\mathbf{p}_i|, \mathbf{0}, q^2) \equiv \frac{\frac{1}{N_{|\mathbf{p}_i|}^{3\text{pt}}}\sum_{\text{fixed}|\mathbf{p}_i|,q^2}\Delta_{t'}C_{PVP}^{3\text{pt}}(t,t';\mathbf{p}_i,\mathbf{0})}{\frac{1}{N_{|\mathbf{p}_i|}^{2\text{pt}}}\sum_{\text{fixed}|\mathbf{p}_i|}C_{PP}^{2\text{pt}}(t,\mathbf{p}_i)[-\Delta_{t'}\partial_{t'}C_{PP}^{2\text{pt}}(t',\mathbf{0}) + E(\mathbf{p}_i)\Delta_{t'}C_{PP}^{2\text{pt}}(t',\mathbf{0})]}, \tag{11}$$

$$R_V^3(t, t'; \mathbf{0}, \mathbf{0}, q^2 = 0) \equiv \frac{\Delta_t\Delta_{t'}C_{PVP}^{3\text{pt}}(t,t';\mathbf{0},\mathbf{0})}{-\Delta_t C_{PP}^{2\text{pt}}(t,\mathbf{0})\Delta_{t'}\partial_{t'}C_{PP}^{2\text{pt}}(t',\mathbf{0}) - \Delta_t\partial_t C_{PP}^{2\text{pt}}(t,\mathbf{0})\Delta_{t'}C_{PP}^{2\text{pt}}(t',\mathbf{0})}, \tag{12}$$

where $q^2 = (\mathbf{p}_i - \mathbf{p}_f)^2 - (E(\mathbf{p}_i) - E(\mathbf{p}_f))^2$. Here, the correlators that are equivalent under cubic rotations are averaged. $N_{|\mathbf{p}_i|,|\mathbf{p}_f|}^{3\text{pt}}$ and $N_{|\mathbf{p}_i|}^{2\text{pt}}$ denote the numbers of correlators to be averaged. For R_V^2 in (11) we can interchange the role of initial and final states and include the case of $|\mathbf{p}_i| = 0$ and $|\mathbf{p}_f| \neq 0$.

Using the expression in (8), it is not difficult to confirm that these ratios $R_V^{k=1,2,3}$ share the same leading order contribution in ChPT, i.e.,

$$R_V^{k=1,2,3}(t, t'; |\mathbf{p}_i|, |\mathbf{p}_f|, q^2) = \frac{B}{Y^2} F_V(q^2) + \cdots. \quad (13)$$

Then, one can eliminate the zero-mode contribution B/Y^2 by taking their ratios. Noting $F_V(0) = 1$, we can extract the form factor through the ratios

$$F_V^1(t, t', q^2) \equiv \frac{R_V^1(t, t'; |\mathbf{p}_i|, |\mathbf{p}_f|, q^2)}{R_V^3(t, t'; \mathbf{0}, \mathbf{0}, 0)}, \quad (14)$$

$$F_V^2(t, t', q^2) \equiv \frac{R_V^2(t, t'; |\mathbf{p}_i|, \mathbf{0}, q^2)}{R_V^3(t, t'; \mathbf{0}, \mathbf{0}, 0)}. \quad (15)$$

They should become independent of t and t' as long as the ground state pion dominates the correlator.

So far we have not given an explicit form of $F_V(q^2)$ in the ϵ expansion since it may contain the physics at higher orders, as well as those beyond ChPT, as explained above. In particular, we do not ignore the pion mass, which appears at the higher order in the ϵ expansion, in the momentum transfer and simply assume the dispersion relation of the pion energy: $E(\mathbf{p}) = \sqrt{\mathbf{p}^2 + m_\pi^2}$ in the following analysis. As shown in the previous section, we expect that inclusion of the mass should not change the analysis very much, as it is a NLO effect. The possible distortion of the dispersion relation due to the NLO finite volume effects will be discussed later.

Because of the zero-mode fluctuation, there is an unusual contribution which includes the scalar form factor of the pion [39]. But this diagram has a pion propagator directly connecting the two pseudoscalar sources, and thus, is expected to be exponentially small. Since the diagram has different t and t' dependences of $F_V^{1,2}(t, t', q^2)$, we can, in principle, numerically confirm if it is really small or not. Here, and in the following, we simply ignore this contribution [we do not observe any unusual t and t' dependences of $F_V^{1,2}(t, t', q^2)$ in the following analysis].

As a final remark of this section, we would like to note that taking ratios is not a new idea but has been widely used for different purposes. The ratio method nonperturbatively cancels the renormalization factors of the operators, makes the effect of excited modes easier to be detected, and so on. Our work shows the ratio (after inserting momenta) is also helpful to remove the dominant part of finite volume effects.

IV. LATTICE RESULTS

We use gauge configurations of size $16^3 \times 48$ generated with the Iwasaki gauge action and $2 + 1$ dynamical flavors of overlap quark action. At $\beta = 2.3$, the value of lattice cutoff $1/a = 1.759(8)(5)$ GeV [$a \sim 0.112(1)$ fm] is obtained using the Ω-baryon mass as an input. The lattice size in the physical unit is thus $L \sim 1.8$ fm.

In this work, we focus on an ensemble with the smallest up-down quark mass, $ma = 0.002$, among a set of ensembles with various sea quark masses. This value roughly corresponds to 3 MeV in the physical unit, and the pion mass at this value is $m_\pi \sim 99$ MeV [42], which is below the physical point. For the strange quark, we choose its mass almost at the physical value, $m_s a = 0.080$. In this setup the pions are in the ϵ regime ($m_\pi L \sim 0.90$), while kaons remain in the p regime.

Along the hybrid Monte Carlo simulation, the global topological charge is fixed at $Q = 0$. Since its effect is encoded in the pion zero mode, the Q dependence does not appear in the ratios of our correlators at the leading order of ChPT.

The correlation functions are calculated using the smeared sources with the form of exponential function. To improve the statistical signal, the so-called all-to-all propagator technique is employed. Namely, the low-energy part of the correlator is calculated from 160 eigenmodes of the Dirac operator and averaged over different source points, while the higher-mode contribution is estimated stochastically with the dilution technique [44]. For Δ_t for the zero-momentum correlator, we use the reference time slice at $t_{\mathrm{ref}} = 12$. For the derivative operator ∂_t, we approximate it by a simple forward subtraction: $\partial_t f(t) = f(t+1) - f(t)$.

We use 148 configurations sampled from 2500 trajectories of the run. The auto-correlation time of the correlators is different depending on the position and momenta. The longest one, from the two-point function with zero momentum, is around 7 trajectories. The statistical errors in the analysis are estimated by the jackknife method after binning data in every 20 trajectories.

Figure 2 presents our lattice data of $F_V^1(t, t', q^2)$ at $(\mathbf{p}_i^2, \mathbf{p}_f^2, \mathbf{q}^2) = (2, 1, 1)$ (top panel) and $F_V^2(t, t', q^2)$ at $(\mathbf{p}_i^2, \mathbf{p}_f^2, \mathbf{q}^2) = (1, 0, 1)$ (bottom panel). The momenta are labeled in the units of $2\pi/L$. The ratio F_V^2 defined in (15) is used when either initial or final spatial momentum is zero with $t_{\mathrm{ref}} = 12$. To estimate $E(\mathbf{p})$, which is involved in the definition of R_V^1 in (10), we use the dispersion relation $E(\mathbf{p}) = \sqrt{\mathbf{p}^2 + m_\pi^2}$. We find a plateau for time separations where t and t' are greater than 5, which is also stable against the change of t_{ref} in the range $9 \leq t_{\mathrm{ref}} \leq 12$ (t_{ref} should satisfy $t + t' + t_{\mathrm{ref}} \ll T$). We fit the data by a constant; the fit results are shown in the plots as well as the fit range.

We plot $F_V(q^2)$ obtained at various q^2 in Fig. 3. They are obtained at various combinations of $\mathbf{p}_i$ and $\mathbf{p}_f$ listed in Table I. For comparison, we also plot the data in the p regime (at $ma = 0.015$) [43]. Apparently, the new data in the ϵ regime show a steeper slope near the origin, which indicates a larger value of the pion charge radius.

We fit the form factor $F_V(q^2)$ to a function

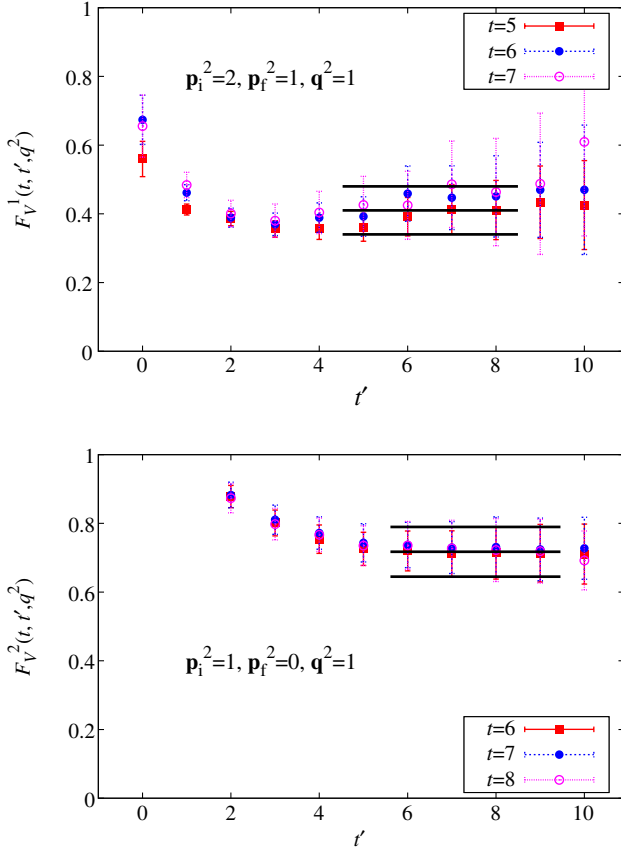$$F_V(q^2) = \frac{1}{1 - q^2/m_V^2} + a_1 q^2 + a_2 (q^2)^2, \quad (16)$$

FIG. 2 (color online). $F_V^1(t, t', q^2 = -0.40 \, [\text{GeV}^2])$ (top panel) and $F_V^2(t, t', q^2 = -0.11 \, [\text{GeV}^2])$ (bottom panel) are plotted as a function of t'. The combination of initial and final momenta are shown in the plots in units of $2\pi/L$. Data for different t's are plotted with different symbols. A constant fit and their error are shown by bands.
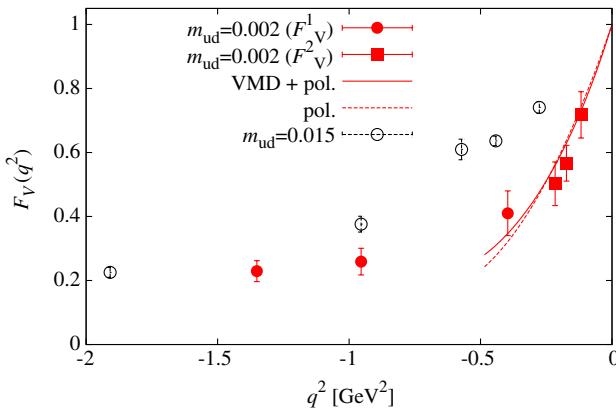

FIG. 3 (color online). Lattice results for $F_V(q^2)$ as a function of q^2. The lattice data in the ϵ regime ($m_{ud}a = 0.002$, filled symbols) and in the p regime ($m_{ud}a = 0.015$, open symbols) are plotted. The ϵ regime data are obtained either from the ratio F_V^1 (circles) or F_V^2 (squares).

TABLE I. Combinations of initial and final momenta taken in the calculation. The momentum components are given in units of $2\pi/L$. Those equivalent under cubic rotations are averaged, though not listed.

$(aq)^2$	$\mathbf{p}_i$	$\mathbf{p}_f$	$\mathbf{q}$
0.0380	$(0, 0, 0)$	$(1, 0, 0)$	$(1, 0, 0)$
0.0560	$(0, 0, 0)$	$(1, 1, 0)$	$(1, 1, 0)$
0.0699	$(0, 0, 0)$	$(1, 1, 1)$	$(1, 1, 1)$
0.1281	$(0, 1, 0)$	$(1, 1, 0)$	$(1, 0, 0)$
0.3084	$(0, -1, 0)$	$(1, 0, 0)$	$(1, 1, 0)$
0.4366	$(0, 0, -1)$	$(1, 1, 0)$	$(1, 1, 1)$

which is motivated by the vector dominance hypothesis and corrections are added as a polynomial. The same function was also used in our previous analysis of the p regime data [3]. Since our calculation of the vector meson mass on the ϵ regime ensemble is too noisy to be useful, we use the physical ρ meson mass, 770 MeV, as an input to (16) and treat a_1 and a_2 as free parameters. The fit curve goes through the lowest four $|q^2|$ points as shown in Fig. 3. The $\chi^2/\text{d.o.f.}$ is below 1.0 in this case. When we include higher $|q^2|$ points, the fit becomes worse and $\chi^2/\text{d.o.f.}$ increases up to 2.5.

The result for the charge radius at our simulated mass is

$$\langle r^2 \rangle_V = 0.63(08)(11) \, \text{fm}^2 \quad (\text{at } m = 0.002), \qquad (17)$$

where the first error is statistical and the second is systematic, as explained below. The central value is larger than the experimental value, $0.452(11) \, \text{fm}^2$.

Although the main part of the pion zero mode's effects is removed, the systematic error due to finite volume remains the dominant one. First, since the momentum space is discrete, the number of data points near $q^2 = 0$ is limited. The choice of the fitting range and/or fitting function affects the determination of the slope at $q^2 = 0$ by 12%. Here we assign the variation of the fit results as the systematic effect. [The central value is taken from the fit of the lowest four $|q^2|$ point to (16).] In addition to the model function (16), we attempt a simple polynomial function of second order (dashed curve in Fig. 3) in this analysis.

Second, the dispersion relation may be distorted in the ϵ regime. By an estimate at the next-to-leading order ChPT, it can be shown that a distortion of the form $E(\mathbf{p}) \to \sqrt{\mathbf{p}^2 + Z_m m_\pi^2}$ with $Z_m \sim 2$ is expected [39]. Since the relation $E(\mathbf{p}) \to \sqrt{\mathbf{p}^2 + m_\pi^2}$ is used when constructing R_V^1, as given in (10), this effect may induce a bias as large as $\sim 10\%$.

Finally, the effect of nonzero modes appeared to be nonnegligible on our small lattice [39]. We estimate its size as 8%. In total, we assign 17% as the total size of the systematic error by adding these sources in quadrature. This is shown in (17) as our estimate of the systematic error.
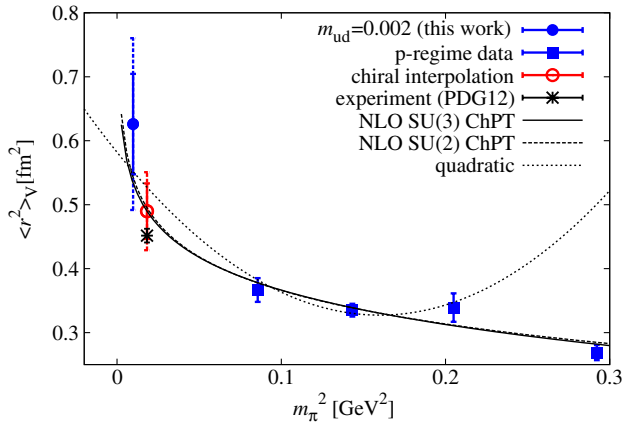
FIG. 4 (color online).   Pion charge radius as a function of m_π^2. A result from this work obtained in the ϵ regime (circle) is plotted together with the data at heavier up and down quarks (square, from [43]). The experimental result is shown at $m_\pi = 135$ MeV. The fit curves are those of next-to-leading order ChPT as well as a simple polynomial (quadratic).

Because it is large, other sources, such as those from discretization effect, are expected to be subdominant.

Figure 4 shows the dependence of $\langle r^2 \rangle_V^\pi$ on the pion mass squared. The result (17) is plotted together with our previous calculation at heavier pions [43]. It is clear that the ϵ regime result (circle) is much higher than the points above $m_\pi \gtrsim 300$ MeV (square). It indicates the existence of the strong (logarithmic) curvature of the pion charge radius near the chiral limit.

Finally, we *interpolate* the data to the physical pion mass. We use the functions suggested by the $SU(2)$ and $SU(3)$ ChPT. At the next-to-leading order, they are

$$\langle r^2 \rangle_V^\pi = -\frac{1}{NF^2}(1 + 6N\ell_6^r) - \frac{1}{NF^2}\ln\frac{m_\pi^2}{\mu^2}, \qquad (18)$$

and

$$\langle r^2 \rangle_V^\pi = \frac{1}{2NF^2}(-3 + 24NL_9^r) - \frac{1}{NF^2}\ln\frac{m_\pi^2}{\mu^2}$$
$$- \frac{1}{2NF^2}\ln\frac{m_K^2}{\mu^2}, \qquad (19)$$

for $SU(2)$ and for $SU(3)$, respectively, with $N = (4\pi)^2$ and F the pion decay constant in the chiral limit. The parameters ℓ_6^r and L_9^r are relevant low-energy constants in $SU(2)$ and $SU(3)$ ChPT, respectively. The result for the charge radius at the physical pion mass is

$$\langle r^2 \rangle_V = 0.49(4)(4) \text{ fm}^2 \quad \text{(at physical point)}, \qquad (20)$$

where the first error is statistical and the second is systematic, including the one in (17) as well as the variation

due to the choice of the chiral fit functions. That includes the ChPT formulas and a polynomial function at the second order.

Through the ChPT fits, we also obtain F and ℓ_6^r (or L_9^r). The value for F is lower than its physical value: 57(8)(10) MeV and 60(9)(9) MeV for the $SU(2)$ and $SU(3)$ fits. This is consistent with our previous extensive analysis of the pion mass and decay constant in two-flavor QCD [45]. The low-energy constants, in the conventional notations, we obtained in this analysis are

$$\bar{\ell}_6 = -6N\ell_6^r(\mu = m_\pi) = 7.5(1.3)(1.5), \qquad (21)$$

$$L_9^r(\mu = 770 \text{ MeV}) = 2.4(0.8)(1.0) \times 10^{-3}. \qquad (22)$$

These values are also smaller than their phenomenological estimates, which may indicate that next-to-next-to-leading order corrections are not negligible, in our p regime data points.

V. DISCUSSIONS AND CONCLUSIONS

In this work, we propose a method to calculate the pion form factor in the ϵ regime. Inserting momenta to the operators, and taking appropriate ratios of them, we can eliminate the dominant contribution from the pion zero mode. A tree-level analysis of the vector pion form factor in the ϵ regime confirms this observation; the result for the pion charge radius is consistent with the experiment, showing the existence of a logarithmic divergence towards the chiral limit.

This cancellation of the zero mode occurs only at the leading order, and there should be nontrivial corrections at the next-to-leading order. This remaining finite volume effects are turned out to be sizable in the presented calculation. On the lattice of size $L \sim 3$ fm or larger, such effect would be reduced to a few % level. One may also use the twisted boundary condition for the valence quarks, although we need a study of the partially quenched effect in the ϵ regime analysis of ChPT.

[1] J. Gasser and H. Leutwyler, Ann. Phys. (N.Y.) **158**, 142 (1984).

[2] J. Gasser and H. Leutwyler, Nucl. Phys. **B250**, 465 (1985).

[3] S. Aoki *et al.* (JLQCD and TWQCD Collaborations), Phys. Rev. D **80**, 034508 (2009).

[4] O. H. Nguyen, K.-I. Ishikawa, A. Ukawa, and N. Ukita (PACS-CS Collaboration), J. High Energy Phys. 04 (2011) 122.

[5] B. B. Brandt, A. Jüttner, and H. Wittig, J. High Energy Phys. 11 (2013) 034.

[6] J. Koponen, F. Bursa, C. Davies, G. Donald, and R. Dowdall, arXiv:1311.3513.

[7] Our preliminary results were presented in Ref. [8].

[8] H. Fukaya *et al.* (JLQCD Collaboration), *Proc. Sci.*, LATTICE2012 (2012) 198 [arXiv:1211.0743].

[9] H. Neuberger, Phys. Lett. B **417**, 141 (1998).

[10] H. Neuberger, Phys. Lett. B **427**, 353 (1998).

[11] P. H. Ginsparg and K. G. Wilson, Phys. Rev. D **25**, 2649 (1982).

[12] M. Luscher, Phys. Lett. B **428**, 342 (1998).

[13] S. Aoki *et al.*, arXiv:1310.8555.

[14] J. Gasser and H. Leutwyler, Phys. Lett. B **184**, 83 (1987).

[15] J. Gasser and H. Leutwyler, Nucl. Phys. **B307**, 763 (1988).

[16] H. Neuberger, Phys. Rev. Lett. **60**, 889 (1988).

[17] H. Leutwyler and A. V. Smilga, Phys. Rev. D **46**, 5607 (1992).

[18] E. V. Shuryak and J. J. M. Verbaarschot, Nucl. Phys. **A560**, 306 (1993).

[19] J. J. M. Verbaarschot and I. Zahed, Phys. Rev. Lett. **70**, 3852 (1993).

[20] J. J. M. Verbaarschot, Phys. Rev. Lett. **72**, 2531 (1994).

[21] P. H. Damgaard, J. C. Osborn, D. Toublan, and J. J. M. Verbaarschot, Nucl. Phys. **B547**, 305 (1999).

[22] P. H. Damgaard and H. Fukaya, J. High Energy Phys. 01 (2009) 052.

[23] F. C. Hansen, Nucl. Phys. **B345**, 685 (1990).

[24] S. Aoki and H. Fukaya, Phys. Rev. D **84**, 014501 (2011).

[25] T. DeGrand, Z. Liu, and S. Schaefer, Phys. Rev. D **74**, 094504 (2006); **74**, 099904 (2006).

[26] C. B. Lang, P. Majumdar, and W. Ortner, Phys. Lett. B **649**, 225 (2007).

[27] P. Hasenfratz, D. Hierl, V. Maillart, F. Niedermayer, A. Schafer, C. Weiermann, and M. Weingart, J. High Energy Phys. 11 (2009) 100.

[28] H. Fukaya *et al.* (JLQCD Collaboration), Phys. Rev. Lett. **98**, 172001 (2007).

[29] H. Fukaya, S. Aoki, T. Chiu, S. Hashimoto, T. Kaneko, H. Matsufuru, J. Noaki, K. Ogawa, T. Onogi, and N. Yamada (JLQCD Collaboration), Phys. Rev. D **76**, 054503 (2007).

[30] H. Fukaya, S. Aoki, S. Hashimoto, T. Kaneko, H. Matsufuru, J. Noaki, K. Ogawa, T. Onogi, and N. Yamada (JLQCD Collaboration), Phys. Rev. D **77**, 074503 (2008).

[31] A. Hasenfratz, R. Hoffmann, and S. Schaefer, Phys. Rev. D **78**, 054511 (2008).

[32] H. Fukaya, S. Aoki, S. Hashimoto, T. Kaneko, J. Noaki, T. Onogi, and N. Yamada (JLQCD Collaboration), Phys. Rev. Lett. **104**, 122002 (2010); **105**, 159901 (2010).

[33] O. Bar, S. Necco, and A. Shindler, J. High Energy Phys. 04 (2010) 053.

[34] F. Bernardoni, P. Hernandez, N. Garron, S. Necco, and C. Pena, Phys. Rev. D **83**, 054503 (2011).

[35] H. Fukaya, S. Aoki, T. W. Chiu, S. Hashimoto, T. Kaneko, J. Noaki, T. Onogi, and N. Yamada (JLQCD and TWQCD Collaborations), Phys. Rev. D **83**, 074501 (2011).

[36] P. Hernandez and M. Laine, J. High Energy Phys. 01 (2003) 063.

[37] L. Giusti, P. Hernandez, M. Laine, P. Weisz, and H. Wittig, J. High Energy Phys. 11 (2004) 016.

[38] P. Hernandez, M. Laine, C. Pena, E. Torro, J. Wennekers, and H. Wittig, J. High Energy Phys. 05 (2008) 043.

[39] H. Fukaya and T. Suzuki, *Proc. Sci.*, LATTICE2013 (2014) 114 [arXiv:1402.2722].

[40] H. Fukaya and T. Suzuki (to be published).

[41] F. Bernardoni, P. H. Damgaard, H. Fukaya, and P. Hernández, J. High Energy Phys. 10 (2008) 008.

[42] H. Fukaya *et al.* (JLQCD Collaboration), *Proc. Sci*, LATTICE2011 (2011) 101 [arXiv:1111.0417].

[43] T. Kaneko *et al.* (JLQCD Collaboration), *Proc. Sci.*, LATTICE2010 (2010) 146.

[44] J. Foley, K. Jimmy Juge, A. O'Cais, M. Peardon, S. M. Ryan, and J.-I. Skullerud, Comput. Phys. Commun. **172**, 145 (2005).

[45] J. Noaki *et al.* (JLQCD and TWQCD Collaborations), Phys. Rev. Lett. **101**, 202004 (2008).